

# Space weather, impacts and forecasting: an overview

**Andrew Sibley<sup>1</sup>,  
Doug Biesecker<sup>2\*</sup>,  
George Millward<sup>2\*</sup> and  
Mark Gibbs<sup>3</sup>**

<sup>1</sup>Operations Centre, Met Office, Exeter

<sup>2</sup>Space Weather Prediction Center, NOAA,  
Boulder, Colorado, USA

<sup>3</sup>Business Services, Met Office, Exeter

## Introduction

There is increasing recognition that disturbances on the Sun can cause problems with Earth-based technology and space instrumentation, especially with the increase in modern applications that utilise sensitive equipment. Air travel is also using new routes that traverse the polar regions where communications are most liable to be disrupted since this is where solar radiation is often focused. The UK Government Chief Scientist, Sir John Beddington, recently commented that we need to start taking the risks associated with 'space weather' seriously because of the vulnerability of modern systems such as the electricity grid and Global Positioning Systems (GPS) that are now widely used for navigation (Alleyne, 2011). The financial cost of disruption from a major event may reach \$2 trillion, but there is also a potential direct human impact in terms of exposure to radiation on long haul polar flights and from the risk of failure of sensitive electronics used in flight control and navigation systems (Baker, 2000; Hall, 2011). Such risks mean that we need to develop effective ways of forecasting space weather events and their level of impact.

This paper provides an overview of the problems associated with space weather and the possibilities for providing forecasting advice. The main emphasis will be on geomagnetic storms, although solar flares and high energy proton events will also be discussed. In one sense the Sun has always

been a major feature of weather forecasting, but as well as visible and ultraviolet light it emits other types of radiation, including very high energy particles and X-rays, and magnetic disturbances from the Sun can interact with the Earth's magnetic field in potentially damaging ways. We will illustrate this overview of the Sun's activity with an example of the (relatively minor) event that took place from 15 to 18 February 2011, as well as that of 28 October 2003 and the very severe Carrington event of September 1859. Several articles have previously been published in *Weather* discussing the possible impacts that space weather may have on the Earth's atmosphere (Toth and Szegedi, 2003; Bushell, 2008; Hall, 2011). Andy Bushell also provided a definition of space weather by referencing wording from The European Cooperation in Science and Technology (COST) Action 724 (Bushell, 2008):

*Space Weather is the physical and phenomenological state of natural space environments. The associated discipline aims, through observation, monitoring, analysis and modelling, at understanding and predicting the state of the sun, the interplanetary and planetary environments, and the solar and non-solar driven perturbations that affect them, and also at forecasting and nowcasting the possible impacts on biological and technological systems.*

## The Sun's characteristics

The visible surface of the Sun, the photosphere, is a cloud of gas about 500km thick with a temperature of around 6000K. It has a bright granular appearance at high resolution due to the presence of numerous very hot areas of rising gas. These bright areas radiate the heat away over a period of about five minutes before the cooler gas descends back into the Sun. Larger dark areas on the surface are sunspots that are sources for most of the activity that concern us. Immediately above the photosphere is the chromosphere, largely consisting of a several thousand kilometre-deep layer of hydrogen and helium gas that gives the Sun its colour during total solar eclipses,

together with cooler visibly-dark gaseous filaments and prominences, and plages (from the French for 'beaches') that are brighter gaseous areas that form above sunspot regions. This layer is best seen in the hydrogen alpha (H $\alpha$ ) part of the electromagnetic spectrum at wavelength 656.3nm. Above the chromosphere is the corona, a very low density, but highly energetic, ionised plasma with temperature typically reaching 10<sup>6</sup>K. The extremely high temperatures, measured in terms of the degree of ionisation, are most probably caused by the intense magnetic field (Barrie, 1994), although the mechanism of heating is still a significant unanswered question in solar physics. In order to monitor the different layers of the Sun from its surface out to the corona it is necessary to study different wavelengths of the electromagnetic spectrum; the Sun's layers are shown by the imagery from the Solar Dynamics Observatory (SDO) (Pesnell *et al.*, 2011) in Figure 1.

The main sources of solar disturbances are sunspots that develop in the photosphere, with associated convection and strong magnetic fields. They are known to emit X-ray flares, high energy proton bursts and Coronal Mass Ejections (CME: see the Glossary at the end of this article for definitions of this and other terms), and develop over a period of days; they vary in complexity through their life span, which is often several weeks. Sunspots show up as dark spots on the Sun's surface due to lower temperatures, typically 3800–4200K, and often have very dark (umbrae) areas within a less dark (penumbra) area (Figure 2). Classification is generally based on size and complexity, using either the Mount Wilson scheme or the McIntosh sunspot classification scheme with modified Zurich criteria (McIntosh, 1990). The most active sunspot regions are ascribed a 'Delta' classification in the Mount Wilson scheme: this is when two umbrae with opposite magnetic polarities exist very close together within a single penumbra. Activity is also related to area as measured in micro-hemispheres (Sammis *et al.*, 2000). Sunspot activity increases and decreases over an approximate 11-year cycle, and we are due another peak in mid-2013. There is also a 22-year cycle

\*The contributions of these authors to this article were prepared as part of their official duties as United States Federal Government employees.

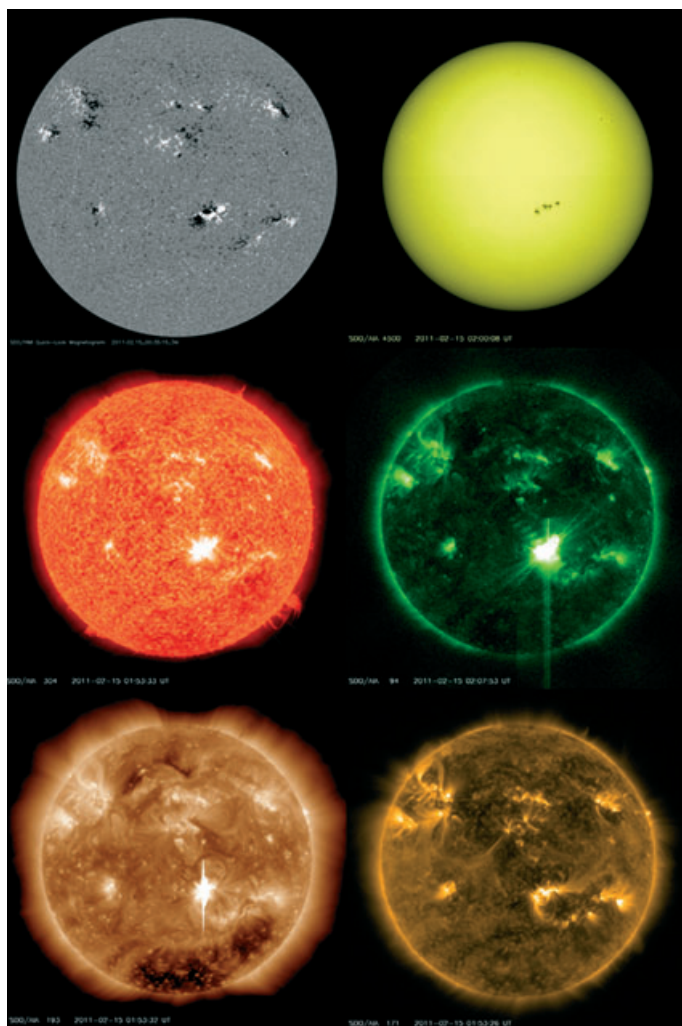


Figure 1. SDO imagery at different wavelengths. From top left to bottom right: HMI Magnetogram, AIA 450nm, 30.4nm, 9.4nm, 19.3nm, 17.1nm. This sequence shows the X ray flare of the early hours (UTC) of 15 February 2011. Courtesy of NASA/SDO and the AIA, EVE and HMI science teams.

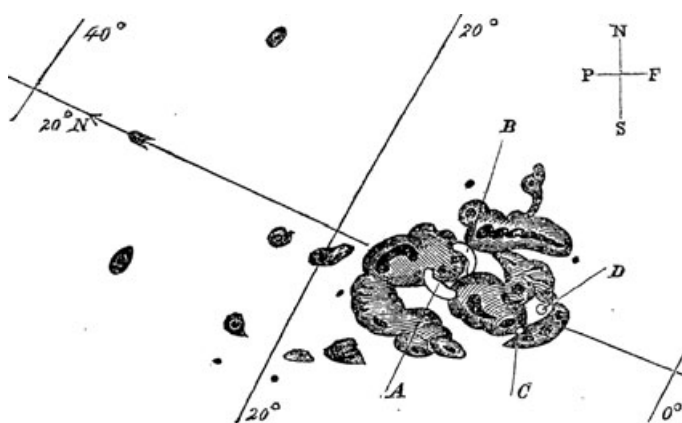


Figure 2. Drawing of very active sunspot region by Carrington (1860), showing umbrae (dark areas) and penumbrae (less dark areas) as observed on 1 September 1859. The white spots A, B show the observed solar flare and movement over a few minutes to C, D.

whereby the polarity of the Sun changes from north to south and back again.

## Monitoring the Sun

The Sun's activity is monitored by a number of satellites, including the geostationary GOES 15, and by many Earth-based instruments and telescopes. Space weather is also

observed using two satellites currently orbiting the Lagrange 1 (L1) orbit: this is about a million miles from the Earth and such that the satellites are able to orbit the Sun and retain their relative (ie effectively near-stationary) position with respect to the Earth. These two satellites are (a) the Solar and Heliospheric Observatory (SOHO) (Domingo *et al.*, 1995), which provides imagery at vari-

ous wavelengths, and (b) the Advanced Composition Explorer (ACE) (Smith *et al.*, 1998) that measures the particle stream and magnetic flux of solar emissions *in situ*. Another platform that has recently been placed in geosynchronous orbit is the SDO satellite, and there are two STEREO (Kaiser *et al.*, 2008) satellites in orbit around the Sun, one travelling ahead of the Earth and the other moving in the opposite direction. These two satellites offer a three-dimensional view of the Sun and allow forecasters to see developments before they move on to the Earth-facing part of the Sun, and to observe the entire volume between the Sun and Earth. Figure 3 shows the position of current satellite platforms. Possibilities for future satellite deployment include locations at the Lagrange 4 and 5 positions: these positions lie on the Earth's orbit, one ahead of and one behind the Earth, and form an equilateral triangle between the Earth, Sun and satellite.

## Solar radio blackouts

Strong X-ray flares are emitted from disturbances that take place in association with very active sunspot regions, usually from Delta spots (Sammis *et al.*, 2000). Such X-ray flares, if they occur on the Earth-facing side of the Sun, are absorbed by the Earth's ionosphere with the focus being centred in that part of the atmosphere directly facing the Sun: that is the equatorial region that lies between the two tropics, although the effect will also be experienced outside of this region as well depending upon the strength of the solar flare. Such X-ray flares travel at the speed of light and arrive at the Earth's surface around 8.5 minutes after emission, causing the Earth's ionosphere to heat up and expand due to the increase in energy in that part directly facing the Sun. The speed of the flare makes forecasting difficult, but the classification of sunspot regions allows forecasters to give a probability of their occurrence and potential size (Sammis *et al.*, 2000). In terms of their impact, a very large X-ray flare may be powerful enough to instantly kill an astronaut outside of the spacecraft (Lilensten and Bornarel, 2006; Bushell, 2008). Figure 4 shows a recent solar flare detected on the GOES 15 satellite, and emitted from NOAA Active Region 1158 on 15 February 2011 around 0200 UTC (referred to as the Valentine's Day event in the American time zone). This was identified as a level R3 flare on the NOAA Space Weather Prediction Center (SWPC) Space Weather Scale (NOAA, 2005), following observation as an X-Class solar flare of intensity of  $2.2 \times 10^{-4} \text{ Wm}^{-2}$ ; it is also shown on the SDO satellite imagery for that time (Figure 1).

The effect of such solar flares on the Earth's atmosphere is to increase the degree of ionisation of the ionosphere and this can cause a number of problems, particularly disruption to communication signals. High frequency



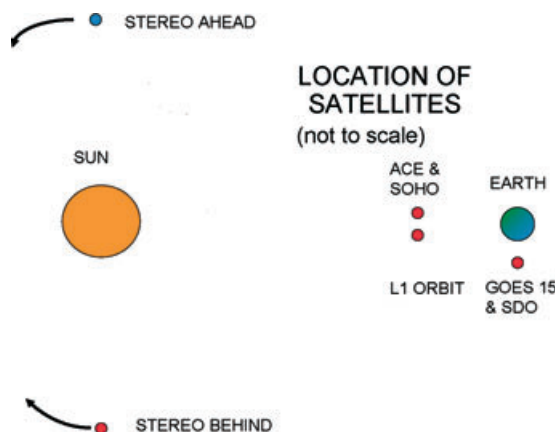


Figure 3. Location of the main satellites used to monitor the Sun. The STEREO satellites are moving slowly behind the Sun.

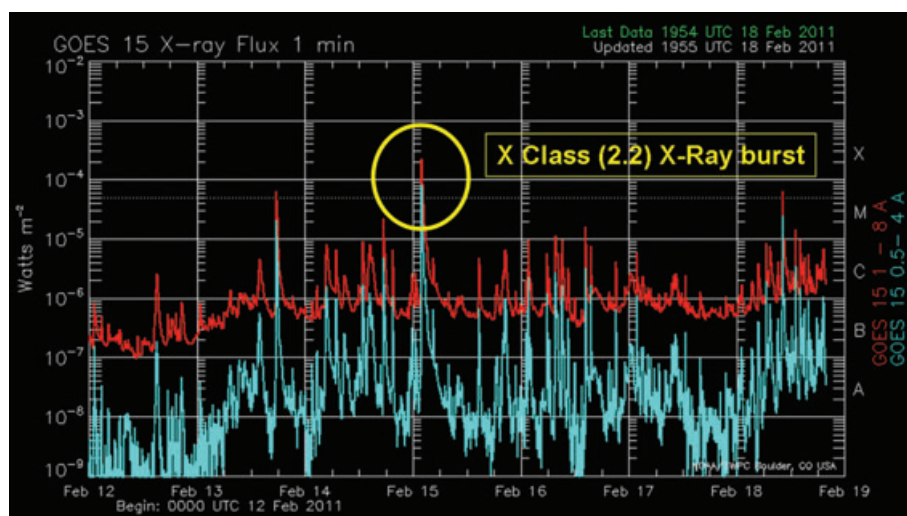


Figure 4. Display of GOES 15 X-ray flux data. This image shows the X Class (2.2) X-ray flare on 15 February 2011. Courtesy of NOAA/SWPC, Boulder, Colorado, USA.

(HF) radio signals are usually refracted through the E Region of the ionosphere (a layer around 100km above the ground), and an increase in the ionisation of atmospheric gases leads to greater signal absorption and thus reduced signal strength, with the potential for loss of contact for shipping and aircraft which rely upon those frequencies; the effect may last for two or three hours. Long-wave, low frequency, navigation signals may also be disrupted due to changes in the height of the ionosphere: such signals are guided around the globe by the ionosphere, typically at a height of around 60–100km. There is also the problem of scintillation with satellite communication as well (this is comparable to the way images are disrupted when viewed through the water of a swimming pool for instance). This effect can, for example, increase errors with Global Positioning Satellites (GPS). Satellites may also suffer from increased drag due to changes in the height of the ionosphere, which has the potential to cause further disruption to communication signals. Figure 5 shows the D Region Absorption Prediction (DRAP) model produced by NOAA SWPC for

28 October 2003 and indicates predicted signal degradation at the level of the D Region (the lowest layer of the ionosphere at around 60km).

## Geomagnetic storms

Although CMEs are often associated with solar flares, they are not the same. They are

caused by the rapid reconfiguration of the magnetic field that is associated with sunspot disturbances, but such disturbances can spread across a large area of the Sun's surface as well. The latest research on CMEs, using the Atmospheric Imaging Assembly (AIA) on the SDO satellite, strongly suggests that they arise from the increased tension in the magnetic field 'ropes' associated with sunspot areas. Magnetic field lines appear semi-circular with the lower half of the loop embedded within the Sun's surface. As such, they tend to be relatively stable and can work to prevent a CME. However, researchers have now discovered a central core around which the magnetic field lines become tightly wound, and it is thought that the increased tension that results allows sufficient energy to build up for an eruption from the Sun's surface. This magnetic rope sets up an electric current which heats the surrounding plasma to a temperature as high as  $10^7$ K. This superheated core first rises relatively slowly, but past a critical point forces a plasma ejection at very high speed (Zhang, 2011) – often in excess of  $1000\text{km s}^{-1}$ . This rapidly-moving plasma cloud can cause problems on Earth if directed towards us, typically some 18–96 hours later; this at least gives forecasters some lead-time to predict the time of arrival. The speed and direction of the CME can be estimated for instance by pictures from the two STEREO satellites (Ahead and Behind); Figure 6 is an image from STEREO Behind showing a growing CME leaving the Sun in the direction of the Earth following the February 2011 flare. On SOHO it is seen as a growing halo (not shown).

Fast CMEs cause a higher pressure shock wave in the solar wind together with their own embedded magnetic field. Subsequent changes to the magnetic field on Earth can cause disruption to power lines and copper-wire communications by inducing unplanned DC currents in the metallic cables (known as Geomagnetically Induced Currents (GICs)); this can overload transformers and other sensitive equipment, though

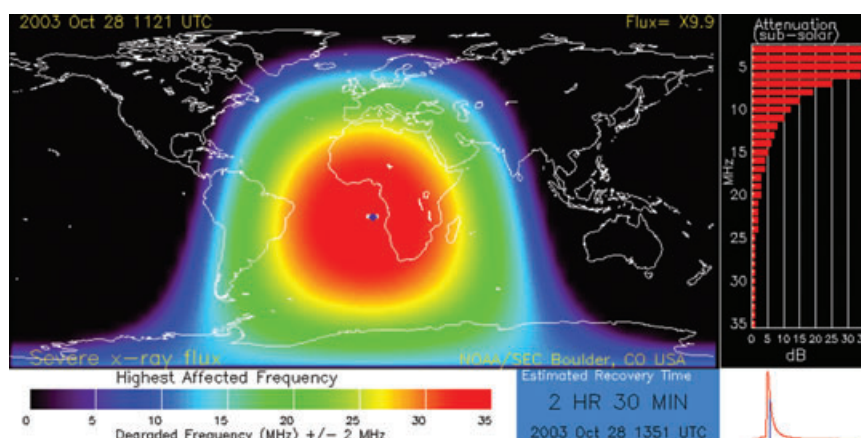


Figure 5. NOAA SWPC model of D Region absorption from X-ray flares. This shows absorption from a flare at 1121 UTC on 28 October 2003, which peaked at  $1.7 \times 10^{-3}\text{Wm}^{-2}$ .

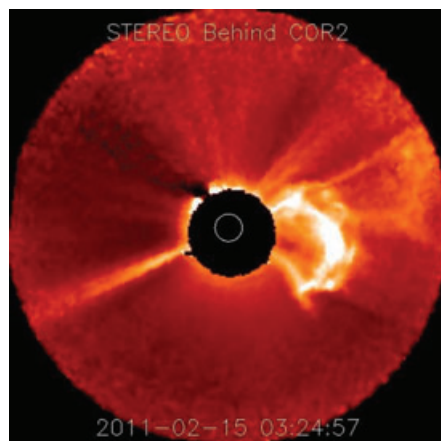


Figure 6. STEREO Behind satellite image showing the CME leaving the Sun at 0324 UTC on 15 February 2011. It arrived at Earth around 72 hours after ejection from the Sun. Information from STEREO satellites can be fed into the WSA ENLIL model (see Figure 9). Courtesy of NASA Goddard STEREO STP science teams.

the effects do depend in part on the configuration of the CME's magnetic field. If the direction of the field is aligned from south to north (that is, in the same direction as the Earth's magnetic field) then linkage of the CME's magnetic field with the Earth's field will be hindered, reducing, though not eliminating, the geomagnetic impacts. However, if the magnetic field of the CME is aligned opposite to the Earth's field (from north to south, a configuration referred to as 'Bz negative'), the magnetic influence is significantly enhanced and the CME is more likely to interfere with the Earth's field and potentially cause disruption at the surface. The ACE satellite provides important information about the magnetic direction (Bz) and size of the CME, but may give a directional forecast lead-time of only 15 minutes for the fastest events, though more typically it is 30–40 minutes. On 15 February 2011, the CME shock wave arrived at the ACE satellite some 72 hours after its onset, at around 0040 UTC. The direction of the magnetic field (Bz) was shown to be towards the north, and there was a jump in density, speed and temperature arising from the solar wind (Figure 7). Figure 8, though, shows a steady increase in the flux of low energy KeV protons ahead of the arrival of the shockwave, and this may provide some useful prior indication for forecasters of the arrival of the CME at the ACE satellite (Smith *et al.*, 2004).

The strength of the effect at the Earth's surface is indicated by magnetometers that measure the size of fluctuations in nano-Teslas (nT); in the UK, the British Geological Survey manages magnetometers at Hartland (Devon), Eskdalemuir (Dumfries and Galloway) and Lerwick (Shetland). The size and direction of the fluctuation determines the strength of the GICs, and for very big events can be of the order of 500nT. Such a

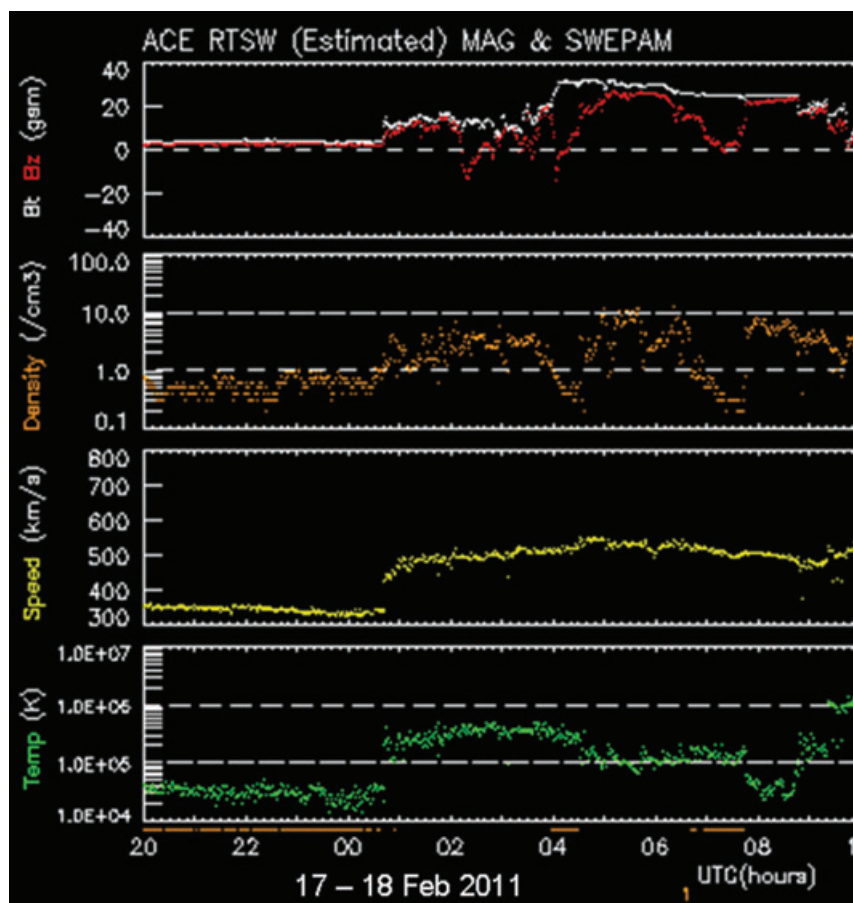


Figure 7. ACE satellite magnetometer and solar wind electron, proton and alpha particle monitor (MAG SWEAPAM). This shows the arrival of the CME around 0040 UTC on 18 February 2011 with a sudden rise in the temperature and speed arising from the solar wind, together with a positive jump in Bz. Courtesy of NOAA/SWPC, Boulder, Colorado, USA.

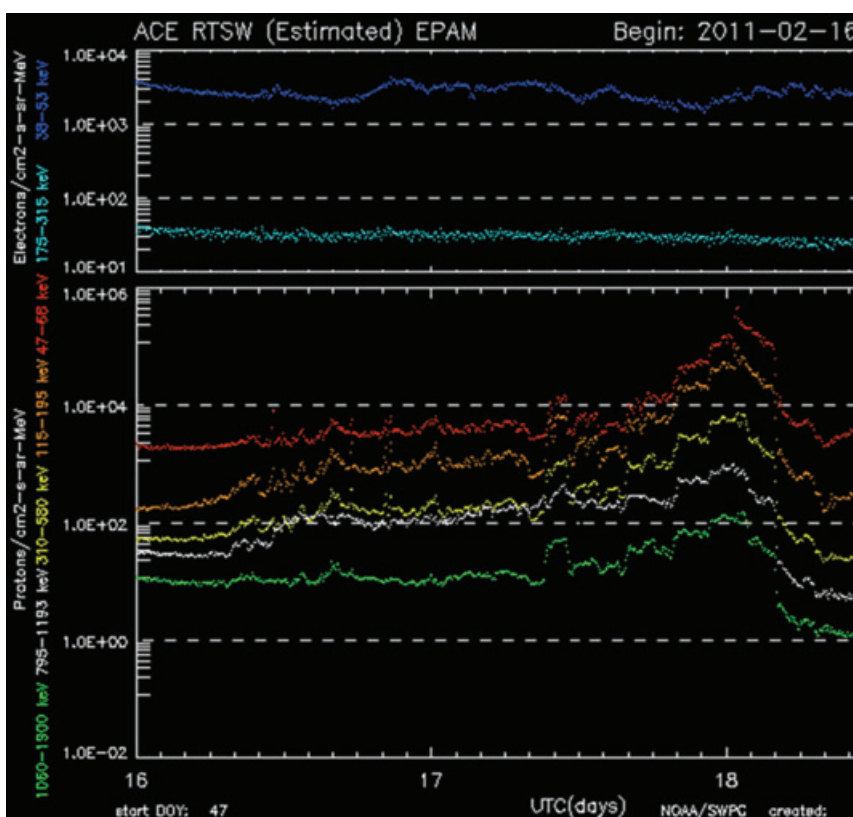


Figure 8. This shows the low energy proton and electrons (EPAM). It shows a slow rise in protons (KeV level) ahead of the arrival of the CME shock wave at the ACE satellite at 0040 UTC 18 February 2011. Courtesy of NOAA/SWPC, Boulder, Colorado, USA.



fluctuation in a magnetometer would represent an extreme G5 Geomagnetic Storm (NOAA, 2005) (although the scale is based upon a planetary (Kp) average measured over a number of geographical locations, and higher latitudes tend to have higher fluctuations). However, Earth-bound magnetometers offer very little prior warning of the scale of effect, which may last many hours. The event in February 2011 had little impact being a relatively weak geomagnetic storm.

One of the largest events in recorded history occurred on 1–3 September 1859 and was responsible for disrupting telegraphic systems across Europe and North America. This has become known as the Carrington Geomagnetic Storm after the astronomer Richard C. Carrington who observed a bright solar flare at around 1120 UTC on the 1st (Carrington, 1860). The event was observed as a projection on stained glass, and was probably a classic two-ribbon flare associated with a CME from a large sunspot group (Figure 2), which was first detected on 26 August 1859 and then drifted across the Sun's surface with multiple eruptions creating effects on Earth that lasted for about a week. The CME is estimated to have taken only 17 hours to arrive, travelling at a speed of some  $2380\text{ km s}^{-1}$ , and was believed to have had a north-south polarity. It caused a great deal of damage to the early telegraph communication systems with a number of telegraph stations reported to have suffered equipment fires due to the strong current induced. A very bright *aurora borealis* was also seen as far south as the

Caribbean (Loomis, 1861). The Carrington storm is thought to have a return period of perhaps 500 years, although there is much uncertainty surrounding such a calculation: it is estimated from nitrate anomalies in ice-core samples, but it is noted that events with half that intensity occur around every 50 years, the last being on 13 November 1960 (Odenwald and Green, 2008).

There are several mathematical models, such as the three-dimensional Wang Sheely Arge (WSA) Enlil model (Odstroicil, 2003), that attempt to determine the CME's progression from the Sun to Earth, although it requires an estimation of initial speed and direction that introduces some uncertainty. They do, though, provide useful guidance to forecasters attempting to predict the size and speed of the CME (Figure 9).

Geomagnetic effects at the Earth's surface can also arise from Coronal Holes. These are regions where the density of the corona is decreased and the magnetic field flows out of the Sun with increased speed together with a stream of charged particles. If a Coronal Hole is directed towards the Earth with the higher-speed solar wind displaying a variable or negative magnetic direction (Bz), then it can cause some minor disturbances to the Earth's magnetic field and produce modest magnetic flux changes in power lines and communication grids.

## Solar radiation storms

Sunspot regions are also thought to be responsible for the high-energy solar radia-

tion storms that may occasionally be directed towards the Earth, although the exact physical mechanism for this effect is uncertain (Reames, 1999). Solar radiation storms are less frequent than other hazards: a strong particle storm (S3) occurs only about 10 times over the 11-year sunspot cycle according to the NOAA Space Weather Scale (NOAA, 2005) and extreme events (S5) occur less than once over the 11-year cycle. Disturbances in sunspot regions accelerate particles, such as electrons, protons and ions, to very high speeds of up to 60% of the speed of light. The severity is dependent upon the proton flux level of particle energy of 10 MeV or above, but they can be as high as 1000 MeV and they are difficult to forecast in advance. Maximum warning time is perhaps of the order of one hour, assisted by the arrival of the less harmful electrons first (Posner, 2007). These particle storms may last for several days, although the highest energy proton events often fade after a few hours. Measurements for Posner's study came from SOHO's COSTEP instrument (Comprehensive Suprathermal and Energetic Particle Analyzer). Figure 10 shows an S1 event, as recorded on the GOES 13 Satellite.

Radiation storms can have negative health consequences for passengers and crew on high-flying aircraft, especially for frequent fliers using the polar routes, as well as increasing the risk of excessive radiation exposure to astronauts (Friedberg and Copeland, 2003). High-frequency communication systems that are used by aircraft for

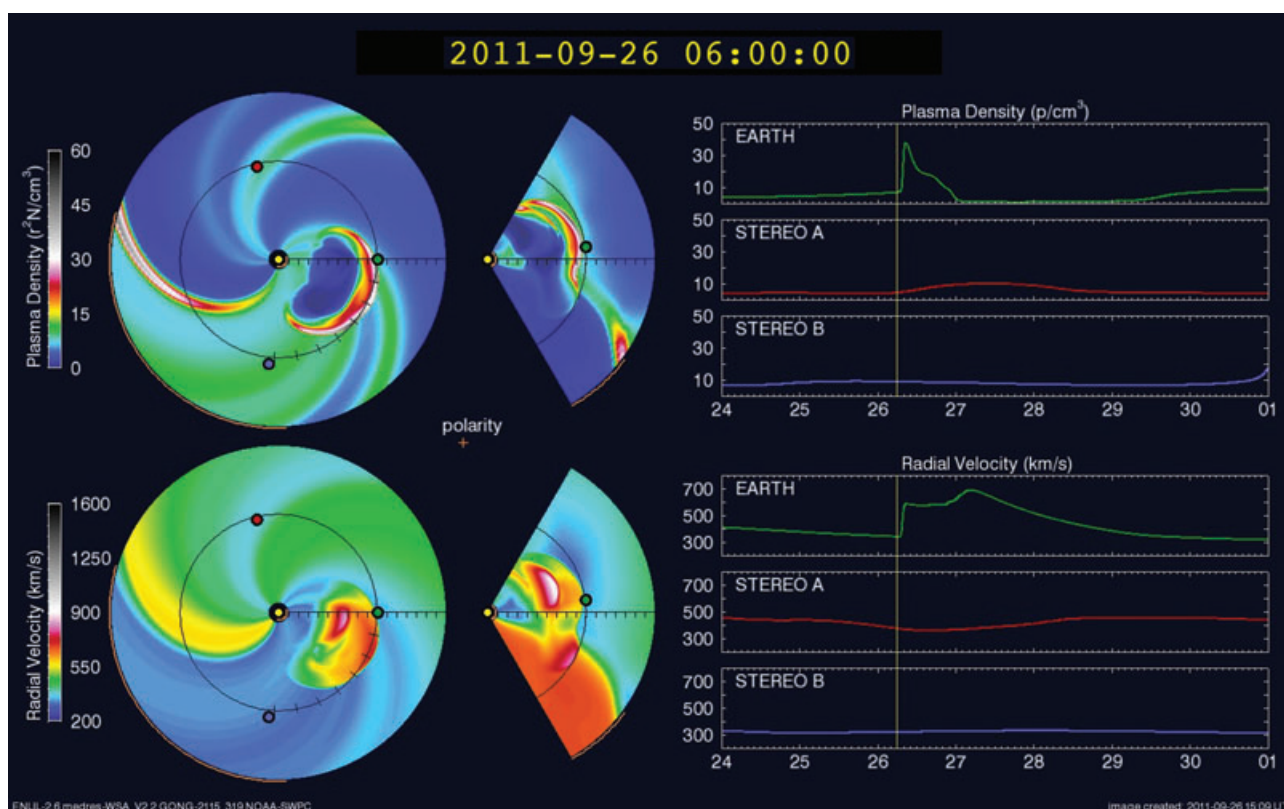


Figure 9. WSA ENLIL model output as run by NOAA SWPC. This is for a CME that arrived at Earth on 26 September 2011.

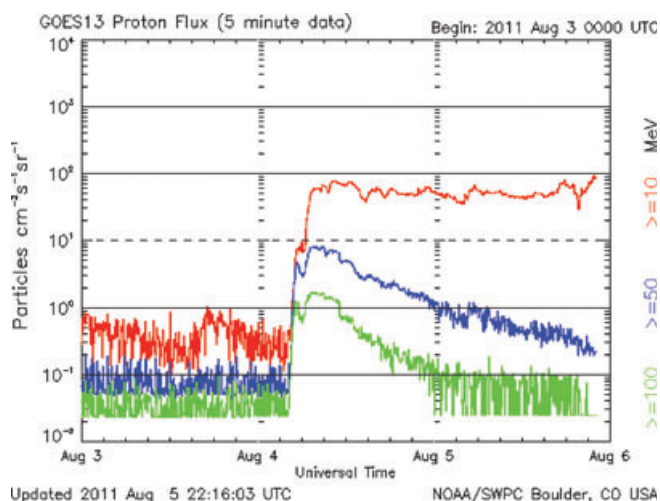


Figure 10. GOES 13 Proton Flux as measured at a level  $\geq 10$  MeV,  $\geq 50$  MeV and  $\geq 100$  MeV. This shows an S1 event on 4–7 August 2011.

navigation can also be disrupted over the polar regions during the more severe events, and delicate instruments on aircraft and satellites may also be damaged as the high-energy charged particles interfere with sensitive equipment through Single Event Upsets (SEU), and degrade solar panels. However, timely warnings of events to aircrew may allow them to descend to lower altitudes or re-route, and warnings to astronauts enable them to take shelter in protected parts of the spacecraft.

## Summary

This has been a brief overview of the hazards presented by disturbances from the Sun, covering the developing science of space-weather forecasting with a focus on geomagnetic storms, but also with some discussion of X-ray flares and high-energy proton events. As well as danger to modern technology there is also a risk to human life and health from such events. Our increasing reliance upon sensitive equipment makes this an important area for continued research, with the aim of improved forecasting techniques. At present forecasting capability is limited because of uncertainties in our knowledge of the activity on the Sun's surface, but the latest satellite imagery, on SDO for instance, offers advances in understanding how the Sun works.

## Acknowledgements

We thank NOAA's Space Weather Prediction Center (SWPC) for their assistance. SDO imagery was provided courtesy of NASA/SDO and the AIA, EVE, and HMI science teams. Thanks are also due to the NASA ACE and STEREO science teams, and to Andy Bushell and David Jackson from the Met Office for additional advice on space weather, as well as to a reviewer for further comments.

## Selected Glossary

**Coronal Mass Ejection (CME).** A mass of charged particles ejected at very high speed from the Sun's corona due to magnetic shock waves. They have embedded magnetic fields and usually come from active sunspot regions.

**Geomagnetically Induced Current (GIC).** A direct current (DC) induced by a changing magnetic field in power cables, telecommunication systems, railway signals and pipelines.

**Lagrange 1 Orbit (L1).** A satellite orbit that is stationary with respect to the Sun and Earth. The L1 position sits about one million miles out from the Earth in the direction of the Sun.

**Solar Flares and Solar Radio Blackouts.** Electromagnetic emissions in the X-ray spectrum from active sunspot regions that are absorbed in the Earth's ionosphere causing radio blackouts.

**Solar Radiation Storms.** Very high energy proton emissions from solar activity that can increase radiation levels for satellites and even at aircraft flight levels.

**Single Event Upset (SEU).** An event where a single proton causes a sensitive electronic system to malfunction.

## References

- Alleyne R.** 2011. Sun Storm May be 'Global Katrina', *The Telegraph*, 27 February <http://www.telegraph.co.uk/science/space/8350329/Sun-storm-may-be-global-Katrina.html> [accessed 10 March 2012].
- Baker DN.** 2000. Effects of the sun on the Earth's environment. *J. Atmos. Sol. Terr. Phys.* **62**: 1669–1681.
- Barrie J.** 1994. *The Stars and the Interstellar Medium: Astronomy and Planetary Science, Book 1*, S281. The Open University: Milton Keynes, UK.
- Bushell AC.** 2008. Space weather: from mud to magnetopause. *Weather* **63**: 244–245.
- Carrington RC.** 1860. Description of a singular appearance seen in the Sun on September 1, 1859. *Mon. Not. R. Astron. Soc.* **20**: 13–15.

**Domingo V, Fleck B, Poland AI.** 1995. SOHO: the solar and heliospheric observatory. *Space Sci. Rev.* **72**: 81–84.

**Friedberg W, Copeland K.** 2003. What aircrews should know about their occupational exposure to ionizing radiation. DOT/FAA/AM-03/16. FAA Civil Aerospace Medical Institute: Oklahoma City, OK.

**Hall B.** 2011. Weather news. *Weather* **66**: 202.

**Kaiser ML, Kucera TA, Davila JM, St. Cyr OC, Guhathakuta M, Christian E.** 2008. The STEREO mission: an introduction. *Space Sci. Rev.* **136**: 5–16.

**Lilensten J, Bornarel J.** 2006. *Space Weather, Environment and Societies*. Springer: Dordrecht, The Netherlands.

**Loomis E.** 1861. On the great auroral exhibition of Aug. 28th to Sept. 4th, 1859, and on auroras generally. *Am. J. Sci.* **82**: 318–335.

**McIntosh PS.** 1990. The classification of sunspot groups. *Sol. Phys.* **125**: 251–267.

**NOAA.** 2005. *NOAA Space Weather Scales*, NOAA SWPC. United States Department of Commerce. [http://www.swpc.noaa.gov/NOAA\\_scales](http://www.swpc.noaa.gov/NOAA_scales) [accessed 10 March 2012].

**Odenwald SF, Green JL.** 2008. Bracing for a Solar Superstorm, *Scientific American*, August, pp. 60–67.

**Odstrcil D.** 2003. Modeling 3-D solar wind structure. *Adv. Space Res.* **32**(4): 497–506.

**Pesnell WD, Thompson BJ, Chamberlin PC.** 2011. The solar dynamics observatory. *Sol. Phys.* **275**: 3–15.

**Posner A.** 2007. Up to 1-hour forecasting of radiation hazards from solar energetic ion events with relativistic electrons. *Space Weather* **5**: S05001. doi:10.1029/2006SW000268

**Reames DV.** 1999. Particle acceleration at the Sun and in the heliosphere. *Space Sci. Rev.* **90**: 413–491.

**Sammis I, Tang F, Zirin H.** 2000. The dependence of large flare occurrence on the magnetic structure of sunspots. *Astrophys. J.* **540**: 583–587.

**Smith EC, Frandsen AM, Mewaldt RA, Christian ER, Margolies D, Ormes JF, Snow F.** 1998. The advanced composition explorer. *Space Sci. Rev.* **86**: 1–22.

**Smith Z, Murtagh W, Smithro C.** 2004. Relationship between solar wind low-energy energetic ion enhancements and large geomagnetic storms. *J. Geophys. Res.* **109**: A01110.

**Toth L, Szegedi S.** 2003. Impacts of space weather on sea-level pressure over the auroral oval. *Weather* **58**: 229–239.

**Zhang J.** 2011. CME cavity, core and flux rope: new insights from SDO and stereo observations. *American Astronomical Society Solar Physics Division Meeting*, Las Cruces, NM, June 12–16.

Correspondence to: Andrew Sibley  
andrew.sibley@metoffice.gov.uk

© British Crown copyright, the Met Office, 2012, published with the permission of the Controller of HMSO and the Queen's Printer for Scotland

DOI: 10.1002/wea.1915